4. Meson-exchange currents and the Δ-isobar

4.1 Introduction

The relativistic framework developed in the previous chapters is used to include the contributions from meson-exchange currents (MEC) and the Δ-isobar, which will also be referred to as two-body currents. The main contributions come from the interference between the Born diagrams and the purely nucleonic diagrams, giving rise to effects which are as large at 50% just below the pion production threshold. In these calculations it is implicitly assumed that we may treat the Δ degrees of freedom in a perturbative way. Treating the Δ-isobar degrees of freedom nonperturbatively in a coupled-channel problem [15] gives similar results, suggesting that a lowest order calculation of the isobar excitation current indeed suffices in the considered kinematic region. Various recent studies exist in the literature using different approaches to investigate these two-body contributions. The results are in general qualitatively similar, but differ in detail in certain kinematic situations, as a consequence of model sensitivity on the chosen dynamics. Our predictions in the considered relativistic one-boson exchange model are found to be of the same order of magnitude as the effects obtained by Gari and Eden [11], using a Hamiltonian formalism. As compared to the results of Jetter and Fearing [12] the importance of the two-body contributions is found to be more enhanced. This is mainly due to the inclusion of a rescaling factor in Ref. [12], introduced to account for the suppression due to rescattering contributions that were not included. We find that the inclusion of the rescattering terms suppresses the effects of the two-body contributions somewhat, but not by the factor of two as was used in Ref. [12].

4.2 Theoretical framework

The observables of the proton-proton bremsstrahlung process can be calculated from the nuclear current. This current can be divided in one-body and two-body contributions [11, 6], where the first gives the major contribution. Within the relativistic description developed in the previous chapters, which included only the one-body contributions, the two-body currents can be incorporated in a perturbative way. These currents can be divided in Born, single- and double-scattering contributions, depicted in Figs. 4.1(a), 4.1(b-c) and 4.1(d),

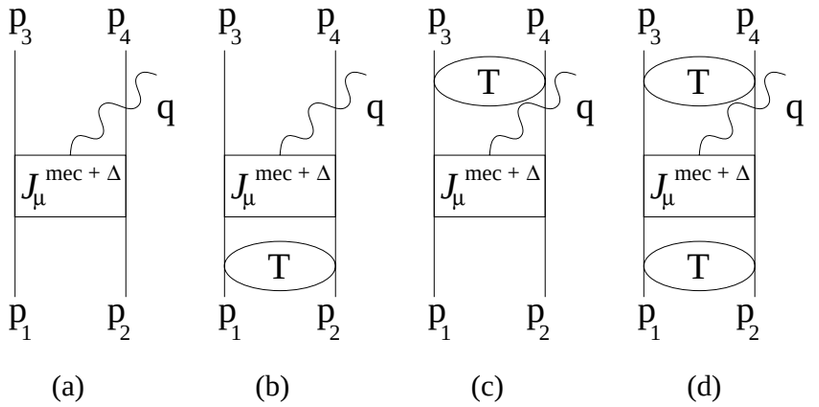

Figure 4.1: *Two-body contributions to the bremsstrahlung current. Diagram (a) is the Born contribution, diagrams (b) and (c) are the single-scattering contributions and diagram (d) is the double-scattering contribution*

respectively.

To write the contributions from two-body currents in a simple form, it is convenient to introduce a two-nucleon scattering state. For the initial nucleons this scattering state is given by

$$\psi(p',p;P) = \left((2\pi)^4\delta^4(p'-p) - iS_2(p',P)T(p',p;P)\right)|p,P\rangle, \tag{4.1}$$

where P and p are the total and relative 4-momentum, $|p,P\rangle$ is the (anti-) symmetrized product of two free Dirac spinors and S_2 is the two-nucleon propagator. A similar expression holds for the outgoing nucleon pair. The T-matrix is determined in the center-of-mass (c.m.) system of the interacting nucleons, and hence the final scattering state can be found from boosting the state from the c.m. system of the final nucleon pair to that of the initial nucleon pair.

With this definition of the two-nucleon scattering state, the current from the sum of all contributions from MEC and Δ currents in the c.m. system of the initial nucleons can be written as

$$J_\mu^{\mathrm{MEC}+\Delta} = \int\int \frac{d^4k'}{(2\pi)^4}\frac{d^4k}{(2\pi)^4}\Lambda(\mathcal{L})\bar{\psi}(p',k';P')\Lambda^{-1}(\mathcal{L})\left(,\,{}^{\mathrm{MEC}}_{\mu} + ,\,{}^{\Delta}_{\mu}\right)\psi(k,p,P), \tag{4.2}$$

where $\Lambda = \Lambda^{(1)}\Lambda^{(2)}$ is the boost from the c.m. system of the final nucleons to the c.m. system of the initial nucleons. P', p' are the total and relative momentum of the final nucleon pair in its c.m. system.

The *NN* interaction is calculated using the Bethe-Salpeter equation, or more specifically, from the Blankenbecler-Sugar [37, 17, 18] (BSLT) 3-dimensional reduction of that equation. We want to make a similar reduction in the integration over the relative energy variables in Eq. (4.2). A consistent choice is to approximate the two-nucleon propagators S_2 in the scattering states ψ and $\bar{\psi}$

by the corresponding BSLT-form:

$$S_2^{\rm BSLT}(p,P) = \frac{1}{2}(E_p - E)\delta(p_0)S^{(1)}(p,P)S^{(2)}(p,P), \tag{4.3}$$

in the c.m. system of the two nucleons. Here $E_p = \sqrt{\boldsymbol{p}^2 + m^2}$ and $2E$ is the total c.m.-energy. With this form for the propagator the integrals in (4.2) reduce trivially to integrations over spatial momenta $\boldsymbol{k}$ and $\boldsymbol{k}'$.

In the present calculation the BSLT approximation for the two-nucleon propagator is used, both in the *NN* interaction and the two-body rescattering contributions. Thus it is assumed that in the integration over the relative energy variable k_0 the only important contributions are coming from the intermediate nucleon propagators, and the contributions from the mesons and the Δ-isobar are ignored. Comparing the quasi-potential results in elastic *NN* scattering with the 4-dimensional Bethe-Salpeter results [16, 21, 28] show that effects of neglecting the k_0 dependence are minor. Furthermore, since the energies discussed here are small as compared to the mass difference of the nucleon and Δ-isobar, it is expected that the contribution from the Δ can be neglected. Another possible reduction scheme for the integration over the relative energy is the equal-time approximation, where it is assumed that the *NN* interaction depends only little on the relative k_0 of the nucleons in its c.m. system, and in effect can be approximated by its value at $k_0 = 0$. Then the integration over k_0 can be done analytically, and the pole-structure is given by the poles in the propagators of the intermediate nucleons and the Δ-isobar. Since the only difference between the equal-time and BSLT approximation is the treatment of the propagators of the intermediate states, this is a possible extension of the present calculation, in which also the contribution of the poles in the Δ-propagator and from the negative-energy states to the integration over the relative energy would be taken into account. Since the rescattering term is relatively small, such an extension would not lead to qualitatively different conclusions.

In the numerical calculation of the remaining 3-dimensional loop integrals in Eq.(4.2) one has to take care of the Green function singularities in a proper way. Below the pion-production threshold the only singularities that occur come from the propagation of the intermediate positive-energy states of the nucleons. As a result of the boosts in Eq. (4.2), the integration is performed in the c.m. frame of the two nucleons. Hence the pole-structure is relatively simple, and these singularities can be removed by standard subtraction methods as described in Appendix B.

4.2.1 Meson-exchange contributions

The contributions from leading-order seagull and pion-in-flight terms vanish in proton-proton bremsstrahlung, since these are proportional to the cross product of the isospin operators of particle 1 and 2. In other words, these contributions vanish because the exchanged mesons are uncharged, and thus the photon does not couple to the mesons. Therefore, the leading-order meson-exchange

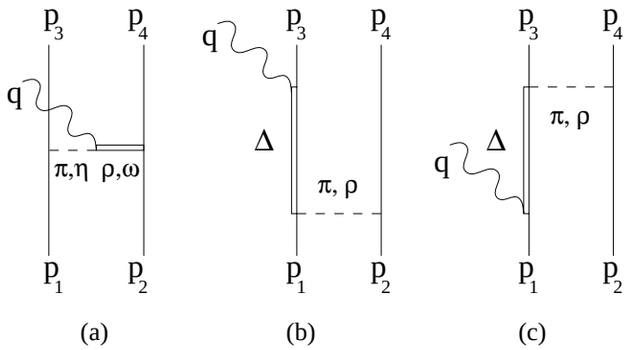

Figure 4.2: *Basic diagrams that enter the calculation of the two-body contributions to the proton-proton bremsstrahlung current: (a) the meson-exchange or meson-decay diagram, (b) and (c) the Δ-isobar contribution.*

currents (MEC) are the decay type diagrams. In the present study the decay of the vector ω and ρ decay into $\pi\gamma$ are included, which are depicted in Fig. 4.2. The decay-contributions of the vector mesons to $\eta\gamma$ are also included, since the extension to these diagrams is simple and they provide a means of estimating the importance of the contributions from heavier mesons.

The couplings of the mesons to the nucleon are the same as in the one-boson exchange that is the kernel of the Bethe-Salpeter equation [37], with the values of the coupling constants as given in Table 4.1. Thus the Lagrangian from the coupling of the pion to the nucleon with mass M is

$$\mathcal{L}_{\pi NN} = -\frac{g_\pi}{2M}\bar{\psi}(x)\gamma_5\gamma_\mu \boldsymbol{\tau}\cdot\partial^\mu\boldsymbol{\pi}\,\psi(x), \tag{4.4}$$

where $\boldsymbol{\tau}$ is the isospin operator. In the case of proton-proton bremsstrahlung actually only the π_0-exchange contributes and hence the third component $\boldsymbol{\tau}$ is relevant. The propagator of the pion is

$$D(k) = \frac{1}{m_\pi^2 - k^2}, \tag{4.5}$$

with m_π the mass and k the momentum of the pion. For the vector mesons the interaction Lagrangians are

$$\mathcal{L}_{\rho NN} = g^{\rm V}_{\rho NN}\bar{\psi}(x)\left(\left(\gamma_\mu - \frac{g^{\rm T}_{\rho NN}}{2M}\sigma_{\mu\nu}\partial^\nu\right)\boldsymbol{\tau}\cdot\boldsymbol{\rho}^\mu\right)\psi(x), \tag{4.6}$$

for the ρ, where $\sigma^{\mu\nu} = \frac{i}{2}[\gamma^\mu,\gamma^\nu]$, and

$$\mathcal{L}_{\omega NN} = g^{\rm V}_{\omega NN}\bar{\psi}(x)\gamma_\mu\boldsymbol{\tau}\cdot\boldsymbol{\omega}^\mu\psi(x), \tag{4.7}$$

for the ω meson. In writing the coupling of the ρ mesons in this way, the constant $g^{\rm T}_{{\rm V}NN}$ measures the strength of the tensor part relative to that of the

	$g^2_{NN}/4\pi$	g^{T}	$g^2_{N\Delta}/4\pi$	m (MeV)
π	14.2		0.35	138.69
ρ	0.43	6.8	4.0	763.0
η	3.09			548.5
ω	11.0	0		782.8

Tab. 4.1: *Meson coupling constants for the NN and $N\Delta$ interactions and the masses of the mesons. For all mesons the cut-off was chosen the same, $\Lambda^2_{NN} = 1.5M^2$ and $\Lambda_{N\Delta} = 910$ MeV. The standard parameters for the $\Delta\gamma$ coupling are $G_1 = 2.51$, $G_2 = 1.62$ and all off-shell parameters are taken to reproduce the on-shell vertices, $Z = -\frac{1}{2}$.*

vector part of the interaction, and for the ω meson this coupling is absent in the present OBE model. The vector meson propagator is

$$D_{\mu\nu}(k) = \left(-g_{\mu\nu} + \frac{k^\mu k^\nu}{m_v^2}\right) D(k), \tag{4.8}$$

where $D(k)$ is of the form (4.5) with the mass of the pion replaced by that of the vector meson. Since the meson-meson-photon coupling does not depend on the isospin operators, the vertex for the decay of either of the vector mesons into the pion and photon can be written as

$$\mathcal{L}_{\mathrm{v}\pi\gamma} = -e\frac{g_{\mathrm{v}\pi\gamma}}{2m_{\mathrm{v}}}\epsilon_{\mu\sigma\nu\tau}F^{\mu\sigma}(\mathrm{v}^\nu\partial^\tau\pi^0), \tag{4.9}$$

where $\mathrm{v} = \rho^0, \omega$, and q and k^{v} are the momenta of the photon and the vector meson, respectively. Only the zeroth component of the ρ and π fields are necessary since the protons exchange only uncharged particles.

The coupling constants $g_{\mathrm{v}\pi\gamma}$ are additional parameters that can be determined from the radiative decay width [38] of the vector mesons,

$$g^2_{\mathrm{v}\pi\gamma} = \left(\frac{4\pi}{e^2}\right)\frac{24,\ (\mathrm{v}\to\pi\gamma)}{m_{\mathrm{v}}(1-m_\pi^2/m_{\mathrm{v}}^2)^3}, \tag{4.10}$$

where again $\mathrm{v} = \rho, \omega$. The width of the ρ^0 is , $= 121 \pm 31$ keV, yielding the coupling constant $g_{\rho\pi\gamma} = 0.23$. For the ω the width is , $= 716 \pm 75$ keV, giving $g_{\omega\pi\gamma} = 0.55$. The uncertainties in the coupling constant are of the order of 10-15%. As can be seen from the derivation of the coupling constants, the relative sign of the ρ and ω coupling is not determined. Here we assume that both couplings have the same sign. Since the main contribution of the meson currents is the result of the ω decay graph, a difference in sign would change the results only little.

The diagrams that contribute to the meson-exchange currents within the present framework are shown in Figs. 4.1(a-d), where the two-body operator for the meson-exchange contributions is given by the diagram in Fig. 4.2(a). To ensure convergence in the integrations over the relative momentum in diagrams 4.1(b-d) and the NN T-matrix, a phenomenological cutoff in the form of a monopole form factor

$$F(k^2) = \frac{\Lambda^2}{\Lambda^2 - k^2}, \tag{4.11}$$

is introduced at each of the meson-nucleon vertices, where Λ is the cutoff mass. In the present OBE-model the cutoff mass, given in Table 4.1, is taken to be the same for all exchanged mesons.

From the interaction Lagrangians as defined above the vertices can be found. These are

$$\begin{aligned}
,_{\pi NN} &= -\frac{g_\pi}{2M}\gamma_5 \not{k}_\pi \boldsymbol{\tau}, \\
,^{\mu}_{\mathrm{v}NN} &= i g^{\mathrm{v}}_{\mathrm{v}NN}\left(\gamma^\mu - \frac{g^{\mathrm{T}}_{\mathrm{v}NN}}{2M}\sigma^{\mu\nu}k_\nu\right) I_{\mathrm{v}}, \\
,^{\mu\nu}_{\mathrm{v}\pi\gamma} &= -i\frac{e g_{\mathrm{v}\pi\gamma}}{2m_{\mathrm{v}}}\epsilon^{\mu\sigma\nu\tau}q_\sigma k^{\mathrm{v}}_\tau,
\end{aligned} \tag{4.12}$$

where I_{v} is τ_3 for the ρ and $\mathbb{1}$ for the ω meson, and $\varepsilon_{0123} = -1$. With the form factors and the couplings as defined above, the general structure for these MEC contributions is given by

$$\begin{aligned}
,^{\mathrm{MEC}}_{\mu} &= -iC_{\pi\mathrm{v}\gamma}\left(\gamma^{(1)}_\lambda - \frac{i g^{\mathrm{T}}_{\mathrm{v}NN}}{2M}\sigma^{(1)}_{\lambda\nu}k^\nu_{\mathrm{v}}\right)\left(-g^{\lambda\sigma} + \frac{k^\lambda_{\mathrm{v}}k^\sigma_{\mathrm{v}}}{m_{\mathrm{v}}}\right) \\
&\quad \times \epsilon_{\mu\alpha\beta\sigma}q^\alpha k^\beta_\pi \gamma^{(2)}_5 \not{k}_\pi I_{\pi\mathrm{v}} + (1 \leftrightarrow 2),
\end{aligned} \tag{4.13}$$

where the numbers between brackets denote the nucleon on which the operator acts. In Eq. (4.13) $I_{\pi\mathrm{v}}$ is now the overall isospin operator, i.e. $\boldsymbol{\tau}^{(1)} \cdot \boldsymbol{\tau}^{(2)}$ for the $\rho\pi$ and $\tau^{(2)}_3$ for the $\omega\pi$ graph. The factor $C_{\pi\mathrm{v}\gamma}$ is

$$C_{\pi\mathrm{v}\gamma} = e g^{\mathrm{v}}_{\mathrm{v}NN} g_{\pi NN}\frac{g_{\mathrm{v}\pi\gamma}}{m_{\mathrm{v}}}F_\pi(k_\pi)F_{\mathrm{v}}(k_{\mathrm{v}})F_{\mathrm{v}\pi\gamma}(q)D_\pi(k_\pi)D_{\mathrm{v}}(k_{\mathrm{v}}), \tag{4.14}$$

where $D_{\pi,\mathrm{v}}$ are the scalar parts of the scalar and vector meson propagators. The strong form factors F_{v} and F_π for the vector and pseudovector meson-nucleon vertices are given by Eq. (4.11). The meson-meson-photon form factor $F_{\mathrm{v}\pi\gamma}$ is unity in the case of real bremsstrahlung ($q^2 = 0$).

For the heavier η meson a similar current can be written. The only difference between the operator structure of the π and η meson is the isospin factor. For the η the factor $I_{\pi\mathrm{v}}$ in Eq. (4.13) is replaced by $\tau^{(2)}$ for the $\rho\eta\gamma$ and 1 for the $\omega\eta\gamma$ graph. The coupling constants are determined in the same way as was done for the pion contributions.

4.2.2 The Δ-isobar contribution

The basic diagrams contributing to the two-body currents of Fig. 4.1, containing an intermediate Δ state are depicted in Figs. 4.2(b-c). Again the NN-meson

vertices and propagators are the same as used in the NN interaction, Eqs. (4.4-4.8). For the Δ propagator the Rarita-Schwinger form is used,

$$\begin{aligned} S_\Delta^{\mu\nu}(p) &= \frac{\not{p} + M_\Delta}{p^2 - M_\Delta^2 + i,\, M_\Delta} \\ &\quad \times \left(g^{\mu\nu} - \frac{1}{3}\gamma^\mu\gamma^\nu - \frac{\gamma^\mu p^\nu - p^\mu \gamma^\nu}{3M_\Delta} - \frac{2}{3}\frac{p^\mu p^\nu}{M_\Delta^2}, \right) \end{aligned} \tag{4.15}$$

where the replacement $M_\Delta \to M_\Delta - i,/2$ is made in order to account for inelasticities due to pion production. For the energy dependence of the width the Bransden-Moorhouse parameterization [39] is used,

$$\begin{aligned} , (q_{\pi N}) &= 0, & q_{\pi N}^2 \le 0 \\ &= \frac{2\gamma (R q_{\pi N}/m_\pi)^3}{1 + (R q_{\pi N}/m_\pi)^2}, & q_{\pi N}^2 > 0, \end{aligned} \tag{4.16}$$

where the momentum $q_{\pi N}$ is defined as

$$q_{\pi N}^2 = \frac{1}{4 s_\Delta} \left(s_\Delta - (m_\pi - M)^2 \right) \left(s_\Delta - (m_\pi + M)^2 \right). \tag{4.17}$$

Here s is the invariant mass of the nucleon-nucleon system and $s_\Delta = (\sqrt{s} - m_N)^2$ is the maximal invariant mass of the Δ. The width , arises from the pole in the πN loop in the propagation of the Δ, giving a contribution only when the invariant mass of the Δ is above the pion-production threshold. Thus below roughly $T_{\rm lab} = 280$ MeV one always has , $= 0$. In Eqs. (4.16-4.17) $q_{\pi N}$ is the maximal 3-momentum available in this self-energy loop under the assumption that the spectator nucleon is at rest. Relaxing this assumption does not lead to significant differences at the energies under consideration [40]. For the adjustable parameters R and γ the values are adopted which give the width of the resonance , $= 120$ MeV at $\sqrt{s_\Delta} = M_\Delta = 1236$ MeV, $R = 0.81$ and $\gamma = 71$ MeV [28]. With this parameterization a good description of the inelasticities in NN scattering is obtained.

The interaction Lagrangians for the coupling of the Δ-isobar to the isovector mesons are used in the form [41]

$$\mathcal{L}_{\pi N\Delta} = -\frac{g_{\pi N\Delta}}{m_\pi} \bar\psi(x) \boldsymbol{T} \psi_\Delta^\mu \partial_\mu \boldsymbol{\pi} + \text{h.c.}, \tag{4.18}$$

for the pion and

$$\mathcal{L}_{\rho N\Delta} = i \frac{g_{\rho N\Delta}}{m_\rho} \bar\psi(x) \gamma^5 \gamma^\mu \boldsymbol{T} \psi_\Delta^\nu (\partial_\mu \boldsymbol{\rho}_\nu - \partial_\nu \boldsymbol{\rho}_\mu) + \text{h.c.}, \tag{4.19}$$

for the ρ-meson, where ψ_Δ is the spin-3/2 Rarita-Schwinger field and $\boldsymbol{T}$ is the isospin operator for the transition of an isospin-1/2 and isospin-1 to an isospin-3/2 particle. From these Lagrangians the interaction vertices can be deduced. However, since the Δ can propagate with both spin-3/2 and spin-1/2, the Δ-vertices can contain additional off-shell terms as compared to the

on-shell forms [42, 43] that follow from Eqs. (4.18) and (4.19). These additional terms reflect the invariance of the total Lagrangian under a contact transformation [44], and as a result the vertices can be written as

$$\begin{aligned} ,^{\mu}_{\pi N\Delta}(k) &= \frac{g_{\pi N\Delta}}{m_\pi}\Theta^{\mu\nu}(Z_\pi)k_\nu, \\ ,^{\mu\nu}_{\rho N\Delta}(k) &= i\frac{g_{\rho N\Delta}}{m_\rho}\left(\not{k}\Theta^{\mu\nu}(Z_\rho) - \gamma^\mu k_\alpha \Theta^{\alpha\nu}(Z_\rho)\right)\gamma_5, \end{aligned} \tag{4.20}$$

for the $\pi N\Delta$ and $\rho N\Delta$ vertices, where Z_α are free parameters. Including the above off-shell structure, the $\gamma N\Delta$ vertex is

$$\begin{aligned} ,^{\mu\nu}_{\gamma N\Delta}(p,q) &= -ie\left(\frac{G_1}{M}\Theta^{\nu\alpha}(Z_1)\gamma^\beta + \frac{G_2}{M^2}\Theta^{\nu\alpha}(Z_2)p^\beta\right) \\ &\quad \times \left(q^\alpha g^\mu_\beta - q_\beta g^\mu_\alpha\right)\gamma_5, \end{aligned} \tag{4.21}$$

with q and p respectively the 4-momentum of the photon and the nucleon. The tensor $\Theta_{\mu\nu}$ is

$$\Theta_{\mu\nu}(Z) = g^{\mu\nu} - (\frac{1}{2} + Z)\gamma^\mu\gamma^\nu. \tag{4.22}$$

For the choice $Z = -1/2$ the tensor $\Theta_{\mu\nu}$ reduces to $g_{\mu\nu}$, and the vertices in Eqs. (4.20-4.21) have the usual on-shell form. This choice will be referred to as the simple coupling scheme. Several other possible choices have been mentioned in the literature [43, 44, 45, 46]. Earlier calculations [12] including this off-shell structure indicate that the amplitude for bremsstrahlung depends only weakly on a simultaneous variation of these off-shell parameters and the coupling constants. This is confirmed in the present calculation, as will be shown below.

4.2.3 Non-relativistic and static limit

With Eq. 4.13 we have a fully relativistic expression for the meson-decay graphs. For intermediate energies often the non-relativistic limit for the meson-exchange currents is used. The expressions for the current in this limit can be found by sandwiching the current between positive-energy states and expanding the resulting expression in orders of p/M, including only the contributions of the lightest mesons (the pion). The static limit corresponds to ignoring the small components in the 4-spinors of the nucleons and the effects of retardation in the operators of the mesons.

To derive the non-relativistic limit, the nucleon spinor is written in the form

$$u(\boldsymbol{p}) = \begin{bmatrix} 1 \\ \frac{\boldsymbol{\sigma}\cdot\boldsymbol{p}}{E+M} \end{bmatrix}\chi(\theta,\phi) \simeq \begin{bmatrix} 1 \\ \frac{\boldsymbol{\sigma}\cdot\boldsymbol{p}}{2M} \end{bmatrix}\chi(\theta,\phi), \tag{4.23}$$

where we have used $E = \sqrt{p^2 + M^2} \simeq M$.

First the static limit reduction of the $NN\pi$ vertex can be performed. In the present model the pion couples through a pseudovector coupling. Since

such a coupling itself contains the momentum $k = p' - p$, the leading-order contribution is proportional to p/M and we can ignore the contributions from the small components of the nucleon spinors. Hence, in the non-relativistic limit the $NN\pi$ vertex is given by

$$\Lambda^{\rm nr}_{NN\pi}(k) = \frac{g_\pi}{2M}(\boldsymbol{\sigma}\cdot\boldsymbol{k}). \tag{4.24}$$

The propagator of the vector meson is given by Eq. 4.8, and reduces in the non-relativistic limit to $-g_{\mu\nu}\Delta_{\rm s}(k)$. The vertex of the ρ mesons consist of a vector part proportional to γ_μ, and a tensor part proportional to $\sigma_{\mu\nu}k^\nu$. The vector part sandwiched between on-shell spinors reduces to

$$\Lambda^{\mu}_{NN\rho} = ig^{\rm v}_{\rho NN}\left(\mathbf{1}\delta^{\mu 0} + \left(\boldsymbol{\sigma}_i\frac{\boldsymbol{\sigma}\cdot\boldsymbol{p}}{2M} + \frac{\boldsymbol{\sigma}\cdot\boldsymbol{p}'}{2M}\boldsymbol{\sigma}_i\right)\delta^{\mu i}\right) + \mathcal{O}\left(\frac{p^2}{M^2}\right). \tag{4.25}$$

This is to be contracted with the meson-decay of the ρ, $\varepsilon_{\mu\alpha\beta\nu}q^\alpha k^\beta$, with Lorentz-structure of the propagator of the meson replaced by $-g^{\mu\nu}$, and the $NN\pi$-vertex. Making use of the commutation relations for the Pauli matrices and the relation between the initial and final momentum, this can be rewritten to

$$,^{\pi\rho\gamma}_{\mu}(v) = iC_{\pi\rho\gamma}\varepsilon_{\mu\alpha\beta\nu}\Big((\frac{\boldsymbol{p}'_i}{2M} + \frac{\boldsymbol{\sigma}^{(1)}\cdot\boldsymbol{k}_{\rm v}}{2M}\boldsymbol{\sigma}^{(1)}_i)\delta_{\nu i} + \delta_{\nu 0}\Big)q^\alpha k^\beta_\rho(\boldsymbol{\sigma}^{(2)}\cdot\boldsymbol{k}_\pi), \tag{4.26}$$

where $C_{\pi\rho\gamma}$ is defined in Eq. (4.14). The anti-symmetric tensor can be used to write the terms as inner and outer products. The product of two Pauli matrices can be written as a single Pauli matrix, giving additional factors i in some of the terms. Thus the contribution to the charge operator from the vector part of the $NN\rho$ interaction is given by

$$\begin{aligned} J_0^{\pi\rho\gamma}({\rm v}) &= \frac{C_{\pi\rho\gamma}}{2M}\Big((\boldsymbol{\sigma}^{(1)}\cdot\boldsymbol{k}_\rho)(\boldsymbol{k}_\rho\cdot\boldsymbol{q}) - (\boldsymbol{k}_\rho\cdot\boldsymbol{k}_\rho)(\boldsymbol{\sigma}^{(1)}\cdot\boldsymbol{q}) \\ &\quad +2i([\boldsymbol{p}'\wedge\boldsymbol{k}_\rho]\cdot\boldsymbol{q})\Big)(\boldsymbol{\sigma}^{(2)}\cdot\boldsymbol{k}_\pi). \end{aligned} \tag{4.27}$$

This operator acts on the nucleon 2-spinors χ. For the contribution to the current operator from the vector part we find

$$\begin{aligned} \boldsymbol{J}^{\pi\rho\gamma}({\rm v}) &= C_{\pi\rho\gamma}\left(\frac{\omega}{2M}\Big((\boldsymbol{\sigma}^{(1)}\cdot\boldsymbol{k}_\rho)\boldsymbol{k}_\rho - (\boldsymbol{k}_\rho\cdot\boldsymbol{k}_\rho)\boldsymbol{\sigma}^{(1)} \right. \\ &\quad \left. +2i[\boldsymbol{p}'\wedge\boldsymbol{k}_\rho]\Big) + i[\boldsymbol{k}_\rho\wedge\boldsymbol{q}]\right)(\boldsymbol{\sigma}^{(2)}\cdot\boldsymbol{k}_\pi). \end{aligned} \tag{4.28}$$

The contribution from the tensor part of the NN-meson interaction can be cast into a similar form as the contribution from the vector part by realizing that

$$-i\sigma_{\mu\nu}k^\nu = \frac{1}{2}(\gamma_\mu\not{k} - \not{k}\gamma_\mu) \simeq (p'+p)_\mu - 2M\gamma_\mu, \tag{4.29}$$

when sandwiched between positive-energy states. Summing the contributions from the vector and tensor part of the NN-meson vertex, the non-relativistic

limit for the contribution from the meson-decay graphs to the charge operator is found to be given by

$$J_0^{\pi\rho\gamma} = \frac{C_{\pi\rho\gamma}}{2M}\Big((1+g^{\rm T})\Big((\boldsymbol{\sigma}^{(1)}\cdot\boldsymbol{k}_\rho)(\boldsymbol{k}_\rho\cdot\boldsymbol{q})-(\boldsymbol{k}_\rho\cdot\boldsymbol{k}_\rho)(\boldsymbol{\sigma}^{(1)}\cdot\boldsymbol{q})\Big)+ +i\Big(([\boldsymbol{p}'\wedge\boldsymbol{k}_\rho]-g^{\rm T}[\boldsymbol{p}\wedge\boldsymbol{k}_{\rm v}])\cdot\boldsymbol{q}\Big)\Big)(\boldsymbol{\sigma}^{(2)}\cdot\boldsymbol{k}_\pi), \quad (4.30)$$

and for the current operator we obtain

$$\boldsymbol{J}^{\pi\rho\gamma} = C_{\pi\rho\gamma}\Big(\frac{\omega}{2M}\Big((1+g^{\rm T})\big((\boldsymbol{\sigma}^{(1)}\cdot\boldsymbol{k}_\rho)\boldsymbol{k}_\rho-(\boldsymbol{k}_\rho\cdot\boldsymbol{k}_\rho)\boldsymbol{\sigma}^{(1)}\big)+ +2i\big([\boldsymbol{p}'\wedge\boldsymbol{k}_\rho]-g^{\rm T}[\boldsymbol{p}\wedge\boldsymbol{k}_\rho]\big)\Big)+i[\boldsymbol{k}_\rho\wedge\boldsymbol{q}]\Big)(\boldsymbol{\sigma}^{(2)}\cdot\boldsymbol{k}_\pi). \quad (4.31)$$

Since we have completely ignored the isospin structure of the NN-meson vertices, the contributions with η or ω mesons is also given by Eq. (4.31), with the substitution of $C_{\pi\rho\gamma}$ by the appropriate constant.

The static limit is found if all terms of higher order in the meson, photon and nucleon momenta are ignored. Thus in the static limit there is no contribution to the charge operator from the meson-decay diagrams, whereas for the current operator the contribution is

$$\boldsymbol{J}^{MEC} = iC_{\pi{\rm v}\gamma}(\boldsymbol{k}_{\rm v}\wedge\boldsymbol{q})(\boldsymbol{\sigma}^{(2)}\cdot\boldsymbol{k}_\pi)+(1\leftrightarrow 2). \quad (4.32)$$

Since the current is purely transversal, only the spatial components perpendicular to the photon momentum are of importance here.

As can be seen from the above expression, the tensor part of the vector-meson vertex does not contribute to the static limit, since it is of higher-order in k/M as compared to the vector part. This holds only for the transversal components of the current. For the charge operator J_0 the tensor part of the interaction enters at the same order in k/M as the vector part. Consequently, in processes such as electron scattering on the deuteron the static limit is known to give a poor approximation [47, 48].

In the present case it is clear that for the ρ-meson, where the tensor coupling is large as compared to the vector coupling, an approximation of the current by the static limit will introduce large deviations from the full result. Hence for these contributions the first-order terms have to be included at intermediate energies. However, since the vector coupling of the ω is much larger than that of the ρ the current from meson-decay graphs is mainly given by the diagrams involving the ω. In the latter case no tensor coupling is assumed to be present. Therefore the static limit might provide a useful approximation in pp bremsstrahlung at intermediate energies. Whether this is indeed the case will be addressed below.

As in the case of the meson-exchange contributions, in the literature sometimes the non-relativistic or static limit is used for the Δ-isobar contributions. Since there are two contributing diagrams, the pre-emission diagram of Fig. 4.2(b) and the post-emission diagram of 4.2(c), the situation is more

complicated than for the meson-decay diagrams. The derivation of the non-relativistic limit for the two contributions is given in Appendix D. For both diagrams it is found that the contribution to the charge operator vanishes in lowest order, whereas the contribution to the current operator from the pre-emission diagram Fig. 4.2(a) is

$$\boldsymbol{J}_i^{\Delta} = \frac{1}{3} C_{\pi\Delta\gamma} P_{\Delta} \Big(2i[\boldsymbol{k} \wedge \boldsymbol{q}] + (\boldsymbol{\sigma}^{(1)} \cdot \boldsymbol{q})\boldsymbol{k} - (\boldsymbol{k} \cdot \boldsymbol{q})\boldsymbol{\sigma}^{(1)} \Big) (\boldsymbol{\sigma}^{(2)} \cdot \boldsymbol{k}), \quad (4.33)$$

where $C_{\pi\Delta\gamma}$ is

$$C_{\pi\Delta\gamma} = e g_{\pi NN} \frac{g_{\pi N}}{m_{\pi}} \frac{G_1}{M_{\Delta}} F_{\pi}(k_{\pi}) D_{\pi}(k_{\pi}), \quad (4.34)$$

and P_{Δ} is the spin-independent part of the Δ-propagator. For the post-emission diagram, Fig. 4.2(b), one has

$$\boldsymbol{J}_f^{\Delta} = \frac{1}{3} C_{\pi\Delta\gamma} P_{\Delta} \Big(2i[\boldsymbol{k} \wedge \boldsymbol{q}] + (\boldsymbol{k} \cdot \boldsymbol{q})\boldsymbol{\sigma}^{(1)} - (\boldsymbol{\sigma}^{(1)} \cdot \boldsymbol{q})\boldsymbol{k} \Big) (\boldsymbol{\sigma}^{(2)} \cdot \boldsymbol{k}). \quad (4.35)$$

In the remainder the sum of the contributions in Eqs. (4.33) and (4.35), retaining the difference between the scalar part of the propagators of the initial and final-state emission diagrams, is taken to be the non-relativistic limit. The static limit is found if furthermore all momentum dependence in the denominator of the Δ propagators is ignored. The resulting expression for the current operator is [49, 50]

$$J^{\Delta} = \frac{4}{3} i C_{\pi\Delta\gamma} \frac{1}{M - M_{\Delta}} [\boldsymbol{k} \wedge \boldsymbol{q}]. \quad (4.36)$$

It is seen that in the static limit there is a large cancellation between contributions from the initial- and final-state emission diagrams. This cancellation depends strongly on the assumption that the difference between the corresponding propagators is negligible. The assumption is only valid when the photon and meson momenta are small compared to the nucleon momentum. As will be seen below, for extreme kinematics at pion-production threshold the difference between the Δ propagators can be as large as 100%.

4.3 Results

As mentioned before, all NN-meson coupling parameters are determined from the OBE-kernel from which the NN interaction is constructed, and the photon-couplings of the mesons were determined from the radiative decay widths. The relevant numerical values for the present calculations are given in Table 4.1.

The contributions from the Δ-isobar intermediate states are less well determined. There is a large uncertainty in the couplings in the $N\Delta\gamma$ vertex, both for the on-shell parameters G_1 and G_2 as well as for the off-shell parameter Z. With the choice of these parameters given in Table 4.1, which are the higher values quoted in the literature [14, 45, 51, 52, 53] without off-shell structure in the vertices, we have calculated the cross section and analyzing power for the bremsstrahlung process just below pion-production threshold, $T_{\rm lab} = 280$MeV. The calculations are done in the lab frame of the initial two nucleon state.

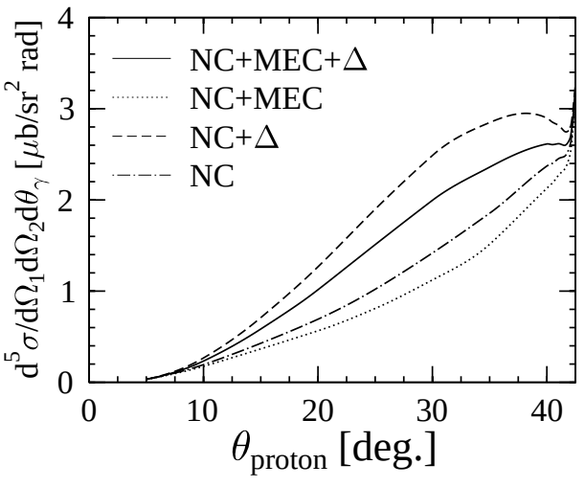

Figure 4.3: *Cross section calculated with the two-body contributions in Born approximation at $T_{\rm lab} = 280$ MeV as a function of equal proton angle $\theta_1 = \theta_2$ for fixed photon angle $\theta_\gamma = 75°$. The full line is the result if both Δ and MEC are included, while for the dotted (dashed) line only the MEC (Δ) contributions are included. For comparison the dot-dashed line shows the result when only the purely nucleonic current are included.*

Figure 4.3 shows the result of a calculation including only the Born diagrams as a function of equal proton angles $\theta_1 = \theta_2$ for fixed photon angle $\theta_\gamma = 70°$. As will be shown below, the Born diagrams give the dominant two-body contributions. Therefore, such a calculation provides a reasonable estimate of the effects of the two-body currents. Comparing the result for the calculation including the two-body currents (the full line) to the purely nucleonic result (the dot-dashed line), it is clear that for these kinematics the contributions from the two-body currents are significant, changing the cross section by as much as 50% at intermediate opening angles. This is primarily due to the Δ contribution, as can be seen comparing the full line to a calculation excluding MEC, the dashed line. From this comparison we furthermore see that the MEC contribution interferes destructively with that of the Δ. Thus in principle both the meson-exchange and Δ currents are significant, and the details of the treatment of these contributions are important, as will be discussed below.

4.3.1 Meson-exchange contributions

The meson-exchange contributions from the single- and double-scattering diagrams are relatively small. This can be seen in Fig. 4.4, where we show the ratio $d\sigma/d\sigma_0$, in which $d\sigma$ is the cross section calculated including the two-body contributions and $d\sigma_0$ is the cross section from the nuclear current of the previous chapters only. The proton angles $\theta_1 = \theta_2 = 23°$ were chosen since just below

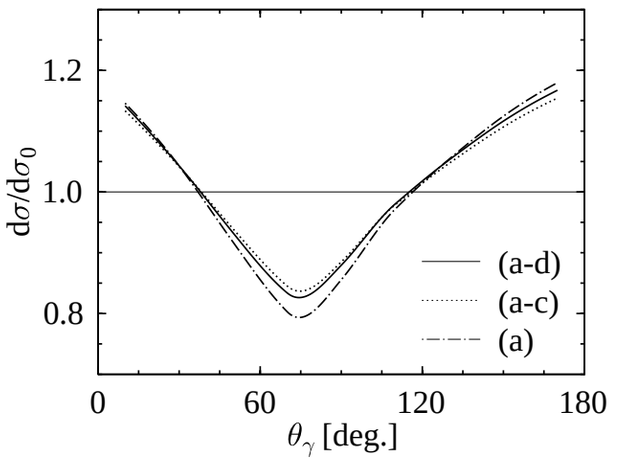

Figure 4.4: *The ratio $d\sigma/d\sigma_0$, where σ_0 is the differential cross section of the previous chapters calculated with only nucleonic contributions and $d\sigma$ is calculated including both nucleonic and meson-exchange contributions at kinematics below the pion-threshold where MEC and Δ contributions are significant ($T_{\rm lab}$ = 280 MeV, $\theta_1 = 27.8°$, $\theta_2 = 28°$). The labeling of the curves show which diagrams of Fig. 4.1 are included. Comparing the calculation including all two-body diagrams (the solid line) and the calculation with the Born and single-scattering MEC (the dotted line) to the calculation including only Born contributions (the dot-dashed line), it is clear that the double-scattering term contributes only little at these energies, whereas the single-scattering contributions give reasonably large effects compared to the Born diagrams. Effects in the analyzing power and other angular combinations are similar.*

the pion-production threshold ($T_{\rm lab} = 280$ MeV) both the relative and absolute size of the contributions from two-body currents are maximal for approximately this combination of angles [12]. The solid line (labeled (a-d)) is the result for the calculation including all meson-exchange diagrams of Fig. 4.1, the dotted line (labeled (a-c)) is the result if only the single-scattering and Born terms are included, whereas the dot-dashed line (labeled (a)) is the result including only the Born contributions. It is seen that the inclusion of the double-scattering diagram changes the overall contribution only by a small amount (of the order of 10% at most). In particular, adding this contribution changes very little in the region where the higher-order contributions play a significant role, between $\theta_\gamma = 50°$ and $\theta_\gamma = 100°$, giving rise to changes up to 30 % of the total effects from meson-exchange currents at $T_{\rm lab} = 280$ MeV. Concluding we can say that the inclusion of the single-scattering contributions to the two-body currents is essential, whereas the rescattering diagrams can be ignored. In what follows we assume that the same conclusions hold for the Δ-isobar contributions to the two-body currents. Since the calculation of the double-scattering graphs

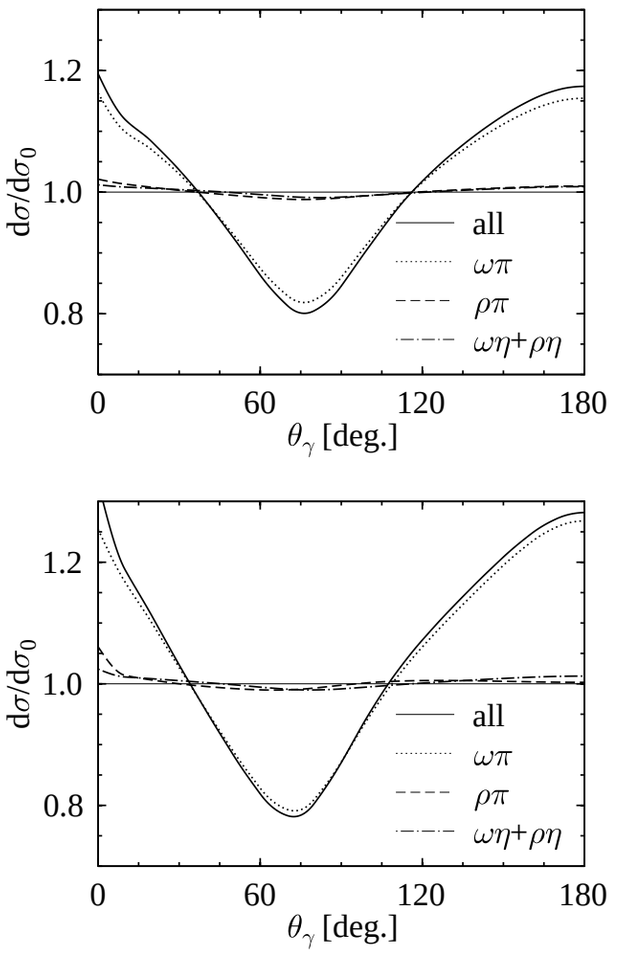

Figure 4.5: *Ratio of the cross sections $d\sigma$ including the different meson-decay graphs and the result $d\sigma_0$ without two-body currents as a function of the photon angle θ_γ at proton angles $\theta_1 = \theta_2 = 23°$ and energies $T_{\rm lab} = 280$ MeV (upper panel) and $T_{\rm lab} = 400$ MeV (lower panel). The most important contribution is the $\omega\pi\gamma$ graph (the dotted line), whereas the $\rho\pi\gamma$ graph (the dashed line) gives a small contribution (less than 5%). The contribution of heavier mesons is of the same order as that of the $\rho\pi\gamma$ graph, as can be seen from the dot-dashed line. The full line is the result if all graphs are included.*

is very time-consuming, we will neglect the double scattering contributions to the two-body currents in the results presented below.

The $\omega\pi\gamma$ is the most important meson-decay contribution. This can be seen in Fig. 4.5, where the ratio of the cross section calculated with the separate MEC contributions ($d\sigma$) to the result when no MEC contributions are included ($d\sigma_0$) is shown as a function of the photon angle θ_γ at proton angles $\theta_1 = \theta_2 = 23^\circ$ and energies $T_{\rm lab} = 280$ MeV (upper panel) and $T_{\rm lab} = 400$ MeV (lower panel). Including the $\omega\pi\gamma$ graph (the dotted line) gives almost the same result as the calculation including all meson-decay contributions (the full line), in particular at intermediate energies. The $\rho\pi\gamma$ graph gives a contribution of at most 5%, as can be seen by comparing the dashed line to the full line. The difference between the size of the contributions from the two vector-meson graphs is primarily due to the relative magnitudes of the coupling constants. To give an estimate for the size of the contributions from the heavier mesons, also the $\omega\eta\gamma$ and $\rho\omega\eta$ graphs were calculated. As can be seen from the dot-dashed curve, these diagrams contribute very little, of the order of a few percent of the $\omega\pi\gamma$ contribution. At the higher energy the contribution is somewhat enhanced, which indicates that the suppression relative to the π-contributions is due to the high mass of the η. Thus at intermediate energies meson-exchange currents with heavier mesons can be ignored.

We have investigated the validity of the static limit for the MEC contributions. Figure 4.6 shows a comparison of a calculation using the full meson-exchange current (the full line) to a calculation with the static-limit approximation to this current (the dotted line). As was seen in Sec. 4.2.3, in the non-relativistic limit the small components of the nucleon spinors are taken into account also, and one would generally expect to find a better approximation of the full relativistic current in this way. The dashed curve in Fig. 4.6 is the result of a calculation using this non-relativistic reduction of the MEC contributions. From the comparison it is clear that for the energies under consideration, the approximation of the meson-exchange currents by the static limit gives deviations of a few percent at most. This is small compared to the contribution itself, as can be seen by comparing the curves to the calculation without meson-exchange contributions (the dot-dashed line). Furthermore, the contributions from small components of the nucleon spinors, i.e. including the first order terms in p/M only gives substantial effects for the analyzing power, in such a way that the non-relativistic limit and the full current give almost identical effects. Clearly for these contributions to the two-body currents the leading-order terms provide a good approximation to the fully relativistic currents.

4.3.2 Δ-isobar contributions

It was found above that the contribution from Δ-isobar currents can be substantial. This is mainly due to the interference between the Δ-currents and the purely nuclear current, whereas the amplitude from the Δ-contributions itself is approximately only 1% of the amplitude from the purely nuclear current.

There is a large uncertainty in the coupling constants for the Δ-contribution,

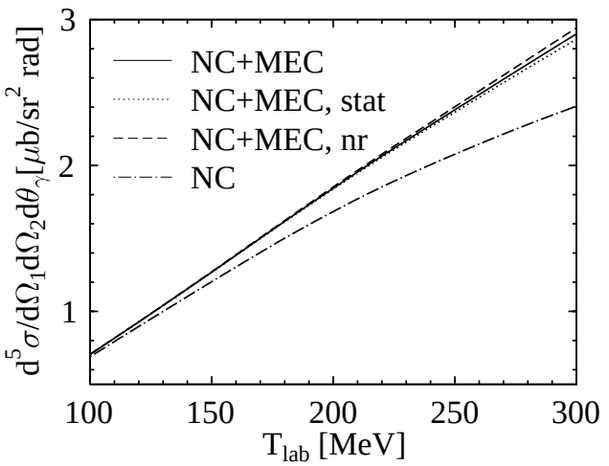

Figure 4.6: *The effect of the static-limit approximation for the meson-exchange currents on the cross section as a function of incoming proton energy $T_{\rm lab}$, for fixed angles $\theta_1 = \theta_2 = 23°$ and $\theta_\gamma = 170°$. The solid curve is the calculation with the fully relativistic currents, the dotted line is the result if we use the static limit, the dashed curve is a calculation with the non-relativistic reduction for the meson-exchange currents (only $\pi\rho$ and $\pi\omega$), and the dot-dashed curve is the result when including only one-body currents.*

with variations as large as 25% in recent literature for the values of G_1 and even larger for G_2. To investigate the influence of this uncertainty in the coupling constants for the Δ contributions, we have done calculations using a number of choices quoted in the literature. Figure 4.7 shows the calculated cross section at kinematics of the TRIUMF [4] experiment where the absolute size of the contributions from the Δ is large, $T_{\rm lab} = 280$ MeV and proton angles $\theta_1 = 28°, \theta_2 = 27.8°$. Various choices of G_1 and G_2, and off-shell parameters Z_γ, Z_π are used. The result without Δ-isobar is given by the dot-dot-dashed line. The full line is the result using the values from a simple vector meson dominance model, where $G_1 = \sqrt{3}\frac{M}{m_\rho}\frac{g_{\rho N\Delta}}{g_{\rho NN}} = 1.9, G_2 = 0$ (the full line). The dotted line is the result when the higher values from Refs. [14, 52], $G_1 = 2.51$, $G_2 = 1.61$ are used, while in both calculation $Z_1 = Z_2 = Z_\pi = -1/2$. The differences in the contribution of the Δ current to the cross section are at most of the order of 20-30%. Similar effects are found in the analyzing power. The Δ contribution shows up mainly as a result of the interference between the Δ and nuclear current, and furthermore the term proportional to G_1 appears to be the most important contribution in the $N\Delta\gamma$-vertex. Therefore, the magnitude of the effect of varying G_1 is in line with what one would expect, since between the two calculations the variation of G_1 is also of the order of 25%.

Variations of the off-shell parameters do not have a significant impact on the size of the Δ-contribution. This can be seen in Fig. 4.7 by comparing the

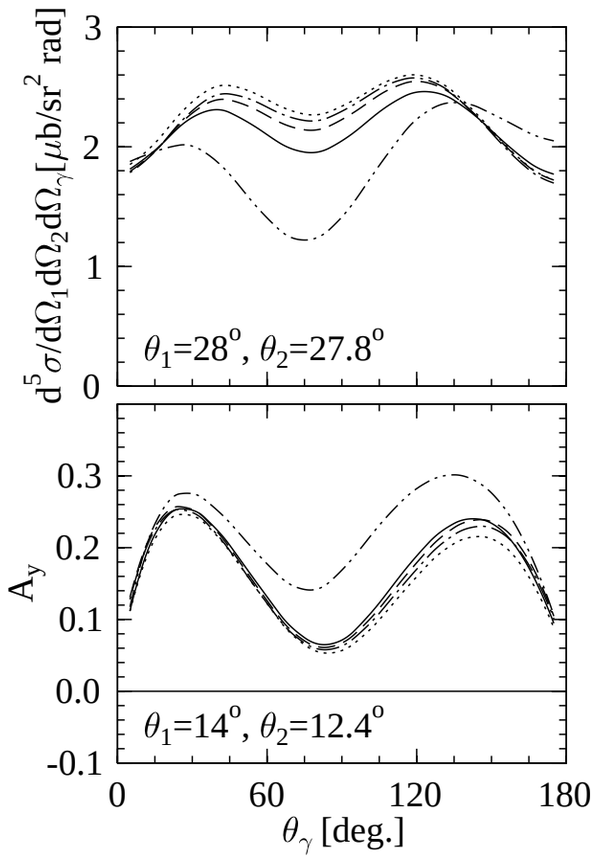

Figure 4.7: *The variations in the Δ-isobar contribution at $T_{\rm lab} = 280$ MeV to the cross section (upper panel) at $\theta_1 = 27.8^\circ$, $\theta_2 = 28^\circ$ and analyzing power (lower panel) at $\theta_1 = 14^\circ$, $\theta_2 = 12.4^\circ$ for different values of the coupling constants and off-shell parameters. $Z_\gamma = Z_\pi = 1/2$ for both full curve, which has $G_1 = 1.9, G_2 = 0$, and dotted curve, which has $G_1 = 2.51$, $G_2 = 1.61$. The dashed curve with $Z_\gamma = 2.25, Z_\pi = 1/2$ and dot-dashed line with $Z_\gamma = 2.25, Z_\pi = -0.346$ both have $G_1 = 2.57, G_2 = 1.22$. For comparison we also show the result when only one-body currents are included (the dot-dot-dashed line). The effects are of the same order as reported in Refs. [15] and [12], and the particular choice of parameters does not influence the general behavior of the effect of the Δ contribution.*

calculation with the values for the coupling constants from Refs. [14, 52] and $Z = -1/2$ (the dotted line) to the result of a calculation using values obtained in a fit to Compton scattering [54], with on-shell parameters $G_1 = 2.57, G_2 = 1.22$ and the off-shell parameters vertex $Z_1 = 0.1, Z_2 = 2.25$ and $Z_\pi = -1/2$ (the dashed curve) or $Z_\pi = -0.346$ (the dot-dashed line). Variations are typically of the order of 10% or less. Thus the particular choice of coupling parameters of the Δ-vertices does not change the general behavior of their contributions. Furthermore the variations found here are similar to the results reported earlier [12, 15]. In the following we use the values quoted in Refs. [14, 52] which are summarized in Table 4.1.

Comparing our calculation to that of Ref. [15], in general the effects of including the Δ contributions is similar to what was found there. The main difference between the two approaches is the absence in the present calculation of the rescattering contribution where the Δ is a spectator. Such a contribution arises primarily from current conservation, and as such is needed only if the Δ is included in the *NN* interaction explicitly.

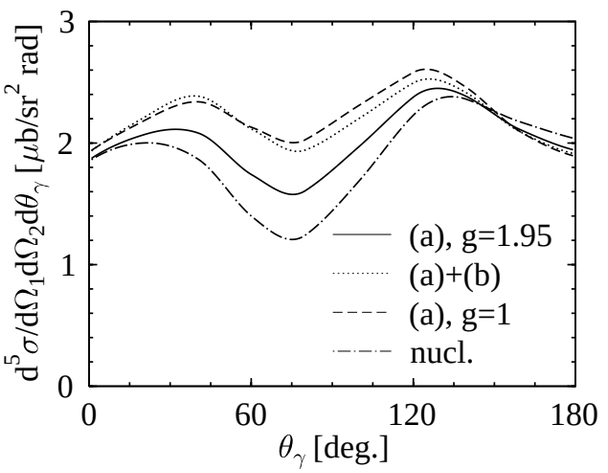

Figure 4.8: *Cross section at $T_{\rm lab} = 280$ MeV, $\theta_1 = 27.8°$ and $\theta_2 = 28°$ as a function of the photon angle θ_γ, calculated using the energy-dependent scaling of the MEC and Δ Born contributions of Ref. [12] (full line, scaling factor $g = 1.95$) compared to a calculation including only the Born without scaling (dashed line, scaling factor $g = 1$) and including both Born and rescattering MEC and Δ contributions (dotted line) and the result for the purely nucleonic current (dot-dashed line).*

In an earlier study of Jetter and Fearing [12] only the lowest order Born contributions were included, while an energy-dependent scaling was introduced to compensate for neglecting higher order terms in the Born series. This scaling factor was deduced from a comparison of the Born results of Ref. [12] with a coupled channels calculation [55]. As was mentioned above, for the meson-decay contributions we find no evidence for the introduction of such a simple

rescaling. To see whether the rescaling might nevertheless provide a useful approximation for the overall two-body current, we have calculated the cross section at $T_{\rm lab} = 280$ MeV, $\theta_1 = 27.8°$ and $\theta_2 = 28°$ using the same approximation, introducing a scaling $g = 1.95$ [12] at this energy. Figure 4.8 shows the comparison of such a calculation (the full line) to a calculation including the Born contributions (Fig. 4.1(a)) without rescaling (the dashed line) and one in which also the single-scattering diagrams (Fig. 4.1(b)) are included (the dotted line). For comparison the dot-dashed line shows the result for the purely nucleonic current. The introduction of a rescaling factor leads to a general suppression of the MEC and Δ contributions. The final result is very similar to the calculations presented in Ref. [12], the difference being the result of the use of a different NN interaction. However, it is clear that the suppression due to the rescattering contributions is overestimated by the simple scaling assumption. In fact the final result is closer to the Born result without scaling, in particular for the Δ-contribution. Furthermore it is seen that the suppression in the calculation including the rescattering contributions clearly depends on the photon angle. Thus from the comparison it is clear that the contributions from the higher order terms at these energies do not yield a simple angle-independent scaling factor.

For the Δ current the static limit implies the assumption that the difference between the denominator of the initial- and final-state propagators can be ignored. A less crude (non-relativistic) approximation is to retain the energy dependence in the denominator, and apply the reduction scheme only to the spin-structure of the Δ contributions. In Fig. 4.9 the upper panel shows the result of the different approximations as function of the energy of the incoming proton, for fixed angles $\theta_1 = \theta_2 = 23°$ and $\theta_\gamma = 50°$, where from previous figures it is clear that the Δ contribution is large. The full line gives the result for the full relativistic Δ current, whereas the dot-dashed line is the result if only the purely nucleonic current is used. As can be seen by comparing this to the dotted line, the static limit does not give a good estimate for energies beyond 150 MeV. The non-relativistic reduction with only lowest-order terms, where the difference in the denominators of the Δ-propagator is retained gives a reasonable estimate up to the pion-production threshold, as can be seen by comparing the dashed curve in the upper panel of Fig. 4.6 to the full relativistic result.

The difference between the full Δ-current and the non-relativistic limit in Fig. 4.9 seems rather large just below the pion-production threshold, but this is because we have chosen the angle such that the difference is maximal. This can be seen from the lower panel in Fig. 4.9 where the same comparison is made as in the upper panel of Fig. 4.9, but now as a function of the photon angle θ_γ at fixed energy $T_{\rm lab} = 280$ MeV. Overall the non-relativistic limit provides a reasonable estimate of the Δ-contribution, whereas the static limit clearly underestimates this contribution. Thus we can conclude that up to the pion-production threshold the static limit is a very poor approximation to the contribution of the Δ, whereas the non-relativistic approximation gives a reasonable order-of-magnitude estimate for the importance of the Δ contribution

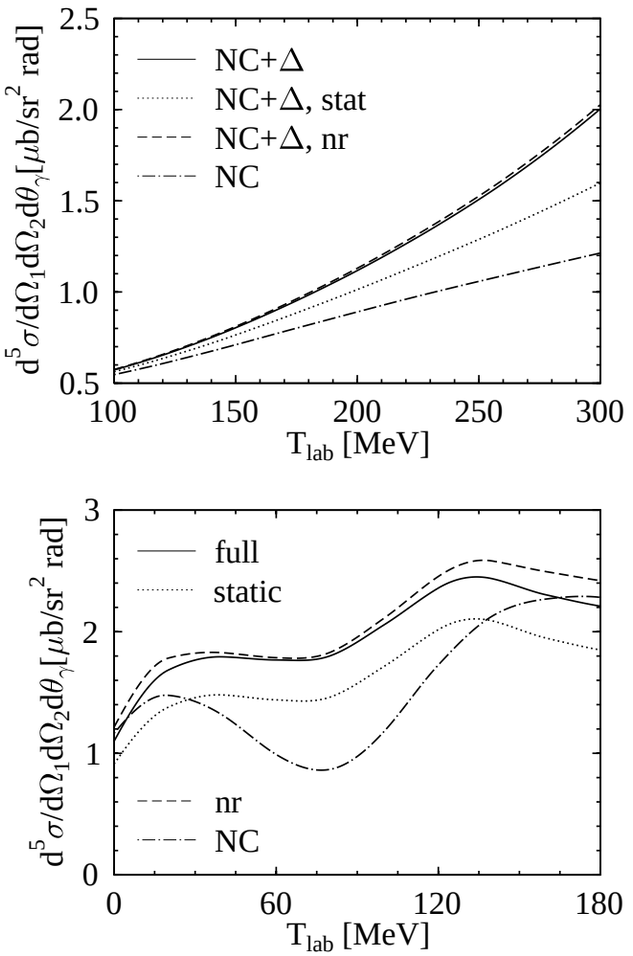

Figure 4.9: *The effect of the static-limit approximation for the Δ-isobar currents on the cross section as a function of incoming proton energy $T_{\rm lab}$ with fixed photon angle $\theta_\gamma = 50^\circ$ (upper panel) and as function of θ_γ for fixed $T_{\rm lab} = 280$ MeV. The proton angles $\theta_1 = \theta_2 = 23^\circ$ are fixed. The solid curve is the calculation with the fully relativistic currents, while the dotted line is the result for the static limit, the dashed curve is a calculation where the energy difference between the Δ-propagators (compare diagrams Fig. 4.2(b) and (c)) is retained. For comparison the result using only the one-body current is given by the dot-dashed curve. Effects in the analyzing power are similar.*

to proton-proton bremsstrahlung.

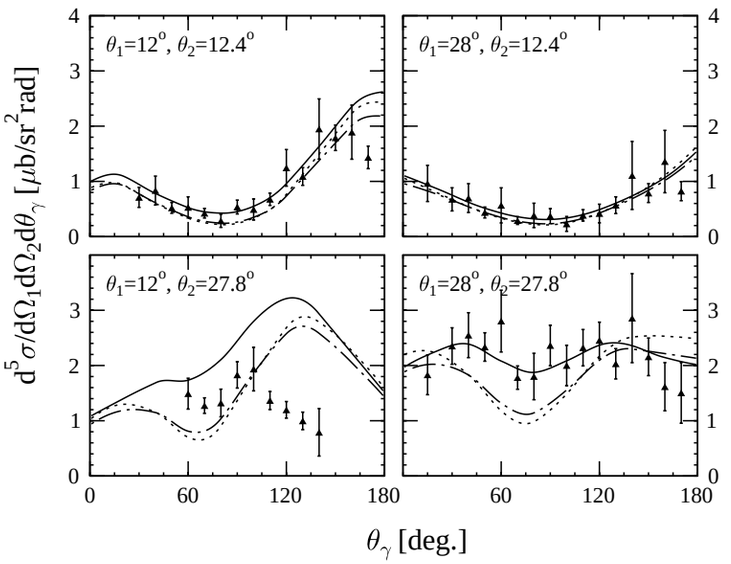

Figure 4.10: *The cross section at $T_{\rm lab} = 280$ MeV as a function of photon angle θ_γ at various proton angles as indicated in the subfigures. The full line is the result of the calculation if both MEC and Δ currents are included, the dotted line if only the MEC contributions are included, whereas the dot-dashed line is the result of the calculation with only the nucleonic current. The data is from the TRIUMF [4] experiment, with the normalization factor 2/3 for the cross section included. Proton 1 is on the same side of the beam as the photon.*

4.3.3 Comparison to experiment

In Figs. 4.10-4.13 we show the cross sections and analyzing powers calculated including the two-body currents for a number of kinematical configurations. Figures 4.10 and 4.11 show the cross sections and analyzing powers at kinematics of the TRIUMF [4] experiment, $T_{\rm lab} = 280$ MeV, as a function of the photon angle θ_γ and for a number of combinations of proton angles. Figure 4.12 shows predictions for the cross section and analyzing power at kinematics of the recent experiment at KVI [8], $T_{\rm lab} = 190$ MeV, as a function of the angle of the protons (respectively θ_1 and θ_2) for fixed photon angle, $\theta_\gamma = 145°$. In Fig. 4.13 the predictions for the cross section and analyzing power at kinematics of the Osaka [9] experiment are shown, $T_{\rm lab} = 400$ MeV, $\theta_1 = \theta_2 = 26°$ and $\theta_1 = \theta_2 = 33°$ as a function of the photon angle θ_γ. In all figures the full and the dotted lines are the results if the Born terms and the single- scattering contributions (corresponding to diagrams 4.1(a-c)) are included with Δ-isobar (full line) and with only MEC (dotted line) respectively. For comparison the

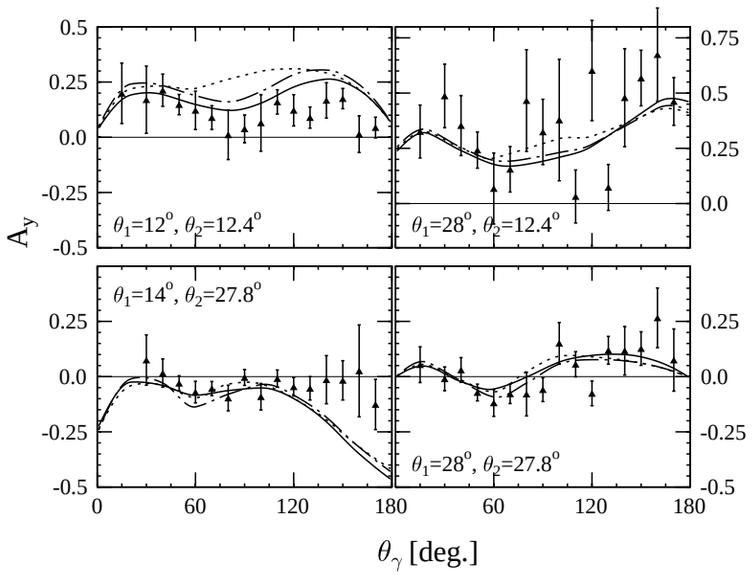

Figure 4.11: *The analyzing power at $T_{\rm lab} = 280$ MeV as a function of photon angle θ_γ at various proton angles as indicated in the subfigures. Curves are labeled as in Fig. 4.10.*

one-body current contribution only of the previous chapters is also shown (dot-dashed line). For all kinematics, the Δ-isobar gives the dominant contribution to the two-body current. The largest effects of the two-body contributions to the current are seen at intermediate proton angles, of the order of $20 - 25°$, while the magnitude of the contributions increase from about maximally 25% at $T_{\rm lab} = 190$ MeV to almost 100% at some specific angles at $T_{\rm lab} = 400$ MeV.

4.4 Conclusions

We have seen that within a relativistic description of *pp* bremsstrahlung, the current conserving two-body currents from meson-decay and Δ diagrams give rise to contributions of the order of 50% to the observables just below the pion-production threshold (at 280 MeV). The main contribution to the two-body current originates from the Δ-isobar currents, resulting in effects in the cross section of at most 75%, whereas the MEC contributions are typically of the order of 10-25% at 280 MeV. The single-scattering contributions to the currents are important, to be contrasted with the double-scattering contributions.

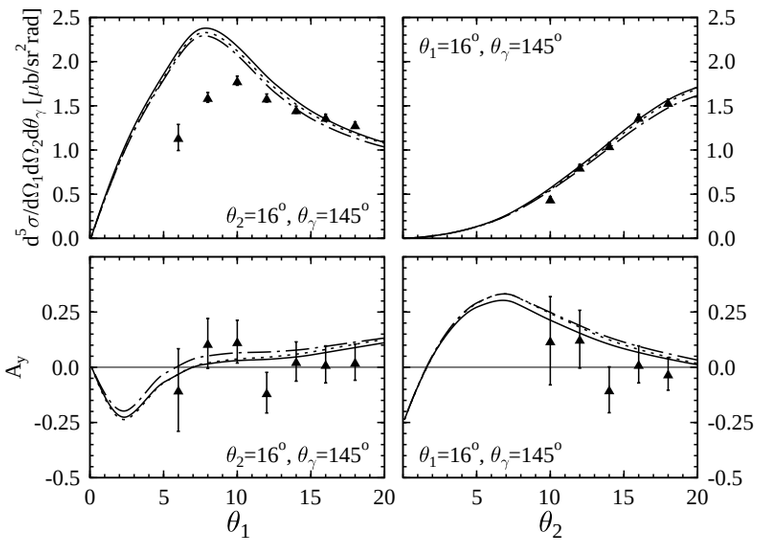

Figure 4.12: *The cross section (top) and analyzing power (bottom) at* $T_{\rm lab} = 190$ *MeV as function of the proton angle* θ_1 *with* $\theta_2 = 16°, \theta_\gamma = 145°$ *(left) and* θ_2 *with* $\theta_1 = 16°, \theta_\gamma = 145°$ *(right). Curves are labeled as in Fig. 4.10. Data is from Ref. [23].*

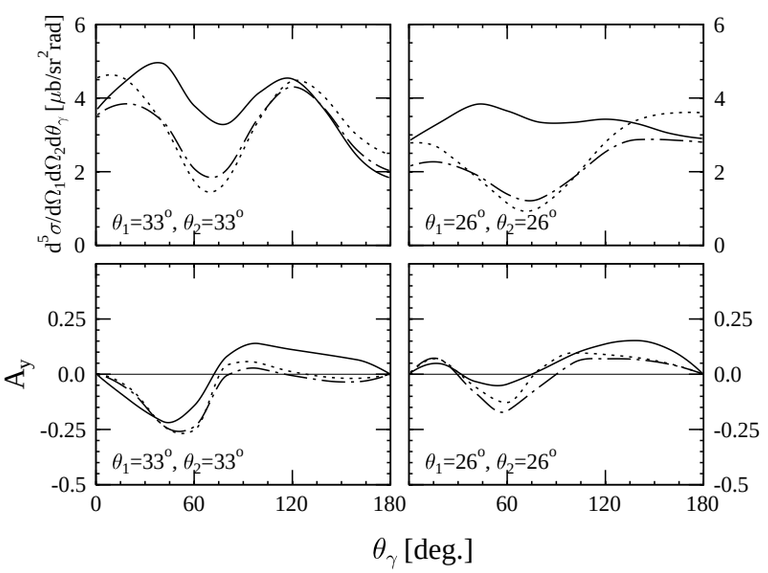

Figure 4.13: *The cross section and analyzing power as function of the photon angle* θ_γ *at* $T_{\rm lab} = 400$ *MeV for equal proton angles* $\theta_1 = \theta_2 = 26°$ *(left) and* $\theta_1 = \theta_2 = 33°$. *Curves are labeled as in Fig. 4.10.*

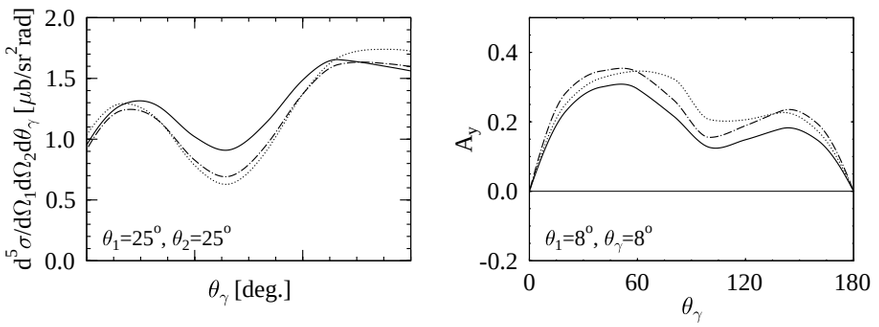

Figure 4.14: *The cross section (upper panel) and analyzing power (lower panel) as a function of the photon angle θ_γ at KVI kinematics ($T_{\rm lab}$ = 190 MeV) for fixed proton angles, $\theta_1 = \theta_2 = 25°$ (cross section) and $\theta_1 = \theta_2 = 8°$ (analyzing power). Including the two-body currents gives effects of at most 25% in the cross section, as can be seen by comparing the full calculation (the full line) to the one which has nucleonic contributions only (the dot-dashed line). The meson-decay contributions tend to cancel the Δ-contributions, most significantly at small and large photon angles.*

The full result of the meson-exchange currents is well reproduced by taking the static limit, which is mainly a result of the dominance of the $\omega\pi\gamma$ contribution. For the $\rho\pi\gamma$ the non-relativistic limit does provide a good estimate of the relevance of this diagram. For the Δ current the static limit gives a very poor order-of-magnitude estimate for the size of this contribution, whereas the non-relativistic limit provides a reasonable order-of-magnitude estimate for the importance of the Δ-contribution to proton-proton bremsstrahlung, showing that it is essential to include the energy dependence of the Δ-propagator.